Author Postprint of the paper published in Physica C 512 (2015) 42–53
The Publisher version can be found at the following doi:10.1016/j.physc.2015.03.005

Measurements on magnetized GdBCO pellets subjected to small transverse ac magnetic fields at very low frequency: Evidence for a slowdown of the magnetization decay.

Jean-Francois Fagnard[a], Sébastien Kirsch[a], Mitsuru Morita[b], Hidekazu Teshima[b], Benoit Vanderheyden[a] and Philippe Vanderbemden[a]

[a] SUPRATECS and Department of Electrical Engineering and Computer Science B28, Sart-Tilman, B-4000 Liège, Belgium
[b] Nippon Steel & Sumitomo Metal Corporation, Futtsu, Chiba 293-8511, Japan

Corresponding author:
Jean-Francois Fagnard
University of Liège, Department of Electrical Engineering and Computer Science B28, Sart-Tilman, B-4000 Liège, Belgium.
E-mail: fagnard@montefiore.ulg.ac.be
Phone: +32 4 366 2674

Abstract

Due to their ability to trap large magnetic inductions, superconducting bulk materials can be used as powerful permanent magnets. The permanent magnetization of such materials, however, can be significantly affected by the application of several cycles of a transverse variable magnetic field. In this work, we study, at $T = 77$ K, the long term influence of transverse ac magnetic fields of small amplitudes (i.e. much smaller than the full penetration field) on the axial magnetization of a bulk single grain superconducting GdBCO pellet over a wide range of low frequencies (1 mHz – 20 Hz). Thermocouples are placed against the pellet surface to probe possible self-heating of the material during the experiments. A high sensitivity cryogenic Hall probe is placed close to the surface to record the local magnetic induction normal to the surface.
The results show first that, for a given number of applied triangular transverse cycles, higher values of $\mathrm{d}B_{\mathrm{app}}/\mathrm{d}t$ induce smaller magnetization decays. An important feature of practical interest is that, after a very large number of cycles which cause the loss of a substantial amount of magnetization (depending on the amplitude and the frequency of the field), the rate of the magnetization decay goes back to its initial value, corresponding to the relaxation of the superconducting currents due to flux creep only. In the amplitude and frequency range investigated, the thermocouples measurements and a 2D magneto-thermal modelling show no evidence of sufficient self-heating to affect the magnetization so that the effect of the transverse magnetic field cycles on the trapped magnetic moment is only attributed to a redistribution of superconducting currents in the volume of the sample and not to a thermal effect.

Author Postprint of the paper published in Physica C 512 (2015) 42–53
The Publisher version can be found at the following doi:10.1016/j.physc.2015.03.005

1. Introduction

Nowadays, powerful permanent magnets can be made of bulk (RE)BCO materials (where RE stands for rare-earth ion) thanks to their ability to trap large magnetic inductions [1-5]. A major issue is to ensure the stability of their permanent magnetization in real application environments. Both theoretical and experimental works have shown that the magnetization of such bulk superconductors can be reduced irreversibly when they are subjected to ac magnetic fields. Two opposite situations can be distinguished: the ac field is either parallel or orthogonal to the magnetic moment. In the parallel configuration, the magnetization decay is well understood and explained by the critical current density reduction caused by the self-heating of the sample due to ac-losses [6-20]. The situation is more intricate when the field is applied transversally to the remnant magnetization [21-42].
This effect, called either "abnormal transverse magnetic field effect", "collapse of the static magnetization" or "crossed-field demagnetisation" was observed on low-T_c wires [21,28,43], bulk (RE)BCO materials [22,25,28,33,34,40], MgB_2 [44] and recently on stacks of 2G tapes [45]. Up to now, however, the exact processes of the magnetization decay in the case of a crossed field configuration are not completely identified. The decay can be due to a redistribution of the superconducting currents in the volume of the superconductor with maybe flux cutting processes but, as it is the case for the axial configuration, a part of this decay might be also due to self-heating of the material subjected to the ac excitation depending on the amplitude and the frequency of the applied transverse magnetic field. Previous experimental and 2D modelling studies [22] have shown that the magnetization decay of superconducting samples subjected to slowly varying transverse magnetic fields of large amplitude is mainly attributed to the modification of the current distribution inside the superconductor and follows a power law as a function of time. In particular, no saturation of this decay was observed after one hundred of cycles of transverse magnetic field. In another study, the suppression of the magnetic moment is shown to be almost independent of the frequency [23] and the trapped field decay can be reproduced qualitatively by calculations based on an isothermal critical state model without any magneto-thermal effects.
The common point of the investigations mentioned above is that they refer usually to a relatively "low" number of transverse ac cycles (typically up to 100-1000) with a "large" amplitude (typically from 0.1 H_p to several times H_p, where H_p denotes the full-penetration field). In applications such as magnetic bearings and brushless ac machines [46-52], however, the transverse fields of small amplitude are applied repeatedly for a long time. This is precisely the regime studied in the present work. An axially magnetized bulk $GdBa_2Cu_3O_7$ (GdBCO) pellet at liquid nitrogen temperature is subjected to a transverse ac magnetic field of small amplitude (typically 5% to 20% H_p) applied for several hours, which corresponds typically to up to 200,000 cycles. The waveform of the parasitic ac field is either sinusoidal or triangular, the latter corresponding to a constant variation of the applied magnetic induction, $|dB_{app}/dt|$. We investigate a wide range of low frequencies (1 mHz – 20 Hz) in comparison to what occurs in pulsed field magnetization process involving dB_{app}/dt of several hundreds of T/s [53,54].

2. Material and methods

The studied sample is a cylindrical bulk single grain $GdBa_2Cu_3O_7$ (GdBCO) pellet from Nippon Steel & Sumitomo Metal Corporation. The dimensions of the sample are 10 mm in height and 15 mm in diameter.

Author Postprint of the paper published in Physica C 512 (2015) 42–53
The Publisher version can be found at the following doi:10.1016/j.physc.2015.03.005

Prior to crossed field experiments, the sample is first characterized experimentally as follows: After being magnetized under 670 mT in « field cooled » conditions, the trapped magnetic induction is measured by Hall probe mapping at z = 500 μm above the sample surface after 15 min, i.e. after the strongest magnetic relaxation effects have taken place [55]. Using such experimental conditions, the sample is nearly fully penetrated (the central area is flatter than expected for a fully penetrated sample) and the magnetic induction at the centre of the top surface equals 450 mT at the contact and is reduced to 380 mT at z = 500 μm as can be seen on the measurement results shown in Fig. 1.

The set-up for the crossed fields experiments consists of (i) an air coil fed by an ac current provided by a KEPCO programmable bipolar power supply controlled by current or voltage (50 V, 20 A, 1 mHz – 400 Hz), (ii) a PVC sample holder to avoid any eddy current and any motion due to the strong magnetic torque that can be induced in the experiments, (iii) a high sensitivity cryogenic Hall probe (Arepoc) placed close to the surface of the GdBCO pellet to measure the local magnetic induction normal to the surface and (iv) two type-T thermocouples placed on the lateral surface at the corner (tc1) and in the median plane (tc2) of the pellet (as figured in Fig. 2) to probe possible self-heating of the material during the experiments. Each thermocouple was glued with a droplet of General Electric varnish (GE 7031), having a thermal conductivity of 0.22 W/mK at 77 K (which is much lower in comparison to the thermal conductivity of the bulk which is roughly 10 W/mK). The thermocouple junction was pressed against the sample surface and insulated from the liquid nitrogen thanks to a layer of varnish, therefore the high convective heat transfer coefficient with the liquid nitrogen was not prevailing in comparison to the conductive heat transfer with the pellet in the value of the thermocouple temperature. The sensor setup and signal waveform are represented in Fig. 2. Note that, for some experiments at the highest frequency investigated (i.e. at 20 Hz), the ac magnetic field is provided by a multifunction synthesizer (HP 8904A) followed by a 2 kW audio amplifier (Crown XTi 2000).

The three procedures (labelled “a”, “b” or “c”) that are used for crossed field experiments are sketched in Fig. 2. The GdBCO sample is magnetized under 670 mT under field cooled conditions (FC). In what follows, “t = 0” is defined as the time at which the magnetizing field is switched off. For all measurements presented in this work, the trapped magnetic induction at the centre of the GdBCO pellet is recorded, starting after 300 s (5 min), for a duration of 1800 s (30 min) to provide experimental data for the natural decrease of trapped field due to flux creep relaxation. A transverse time-varying magnetic field is then applied at t = 2100 s for a given time. In procedure (a), only one cycle is applied, while in procedures (b) and (c), a large number of bipolar cycles are applied, with either sinusoidal (b) or triangular (c) waveforms.

3. Theory/calculation

Assuming that the electric field E varies with the current density as a power law:

$$E(J) = E_c (J/J_c)^n \quad , \tag{1}$$

where n is the critical exponent (Zeldov model), the decay of the superconducting current (and therefore of the remnant induction) reads:

Author Postprint of the paper published in Physica C 512 (2015) 42–53
The Publisher version can be found at the following doi:10.1016/j.physc.2015.03.005

$$J(t) \approx J_{c0}\left[1 - \frac{1}{n}\ln\left(\frac{t}{t_0}+1\right)\right]. \quad (2)$$

In the literature, this decay law is sometimes approximated by a power law given by:

$$J(t) \approx J_{c0}\left[1+\frac{t}{t_0}\right]^{1/(n-1)}. \quad (3)$$

We call "natural relaxation" of the superconducting currents (or the trapped field by extension), the decay of the superconducting currents due to the flux creep process described by Eq. (2). This natural relaxation is to be contrasted with the decay of the superconducting currents (or the trapped field) due to an external cause like, in the case of this paper, the application of a transverse ac magnetic field. In this work, we use Eq. (2) to extrapolate the natural relaxation of the trapped field using only the data recorded between t = 300 s and t = 2100 s where no external magnetic field is applied. In order to check the validity of the logarithmic law for larger times, several measurements of the trapped field decay were carried out for several hours without external magnetic field. These measurements were compared to the extrapolated values obtained from Eq. (2) which was fitted to experimental data only between t = 300 s and t = 2100 s. The discrepancy between experimental measurements and extrapolated values was found to be less than 1%.

Numerical modelling is carried out with an open-source finite element solver (GetDP) developed in the Applied and Computational Electromagnetics research unit of the University of Liège. A complete description can be found in [56-58]. The model is based on an isotropic $E(J)$ power law (cf. Eq. (1)) and a $J_c(B)$ relationship described by Kim's law :

$$J_c(B) = \frac{J_{c0}}{1+B/B_0}. \quad (4)$$

It is solved in 3D with an H- formulation. We emphasize, however, that this model neglects effects related to potential longitudinal currents and for which the used constitutive equations may no longer be valid. Therefore, care should be taken in interpreting the 3D results.

In order to discuss the thermal behaviour of the superconducting pellet, we have first to calculate the Biot number which is the dimensionless number comparing the convective and the conductive heat transfer of a material in a given environment. The Biot number is defined by $Bi = U*L_c/k$ where U is the convective heat transfer coefficient, L_c is a characteristic length of the pellet (here the half-height, i.e. 5 mm) and k is the thermal conductivity, assumed to be isotropic. In reality, the thermal conductivity is also anisotropic due to the layered structure of the REBCO materials. According to several references in the literature, the thermal conductivity along the c-axis ranges between 2 and 10 W/mK while the values reported for the thermal conductivity in the ab-planes is between 10 and 20 W/mK [10, 59-61]. On the other hand, the convective heat transfer coefficient values depends strongly on the experimental conditions and on the temperature gradient between the coolant and the superconductor. In low pressure cryogenic gas or in vacuum, the convective heat transfer coefficient is small, as an example a value of 1.94 W/m²K is reported in [62] while when in cryogenics fluids, it can be several orders of magnitude larger. In addition, in liquids, several

heat draining regimes exist (free convection, nucleate boiling, transition boiling and film boiling) which correspond to several overall convective heat transfer coefficients [64]. In the case of liquid nitrogen, the convective heat transfer coefficient equals 2000 W/m²K for small temperature differences between the coolant and the superconductor and it can increase to values of 13000 W/m²K for larger temperature differences [10, 63-64].

Considering the values of k and U found in the literature, the lowest Biot number for the sample studied in our paper is equal to 0.5 for k = 20 W/mK and U = 2000 W/m²K and the highest Biot number equals 32.5 for k = 2 W/mK and U = 13000 W/m²K. Therefore, we have decided to carry out 2D magneto-thermal modelling with various thermal parameters to calculate the temperature distribution inside the superconducting pellet to estimate its effect on the demagnetization of the superconducting pellet.

The model is based on the Brandt algorithm on an infinite bar first magnetized along the y-direction (representing the c-axis of the sample) and subsequently subjected to an AC magnetic field in the x-direction. The constitutive laws used in the model are an $E(J)$ power law with a creep exponent n and a field and temperature dependent J_c by using a Kim law whose both parameters, J_{c0} and B_0 are linearly temperature dependent. Unfortunately this model does not allow to consider anisotropic J_c. The thermal behaviour is taken into account in the modelling by considering the – isotropic or anisotropic – thermal conductivity of the sample and the convective heat transfer coefficient between the sample and the liquid nitrogen. These parameters control the dissipation of the heat generated inside the superconductor during the application of the transverse AC magnetic field. All the 2D magneto-thermal modelling results are obtained in the case of an AC magnetic field of 50 mT applied at 20 Hz, which corresponds to the strongest amplitude and highest frequency studied experimentally in our paper.

4. Results

In all experiments presented in this paper, the GdBCO pellet is axially magnetized under 670 mT (in field cooling conditions) and the maximum trapped magnetic induction measured at 0.5 mm from the surface (after 15 min) is found to be 450 mT. The axial full penetration field was measured to be $\mu_0 H_p$ = 1.15 T at 77 K.

4.1. Influence of the sweep rate on the decay of the trapped field

The first experiment is carried out as follows: at t = 2100 s after the end of the axial magnetization process (cf. Fig. 2(a)), a transverse magnetic field pulse of triangular waveform is applied in order to carry out measurements at given $|dB_{app}/dt|$. The maximal amplitude of the triangular pulse of the applied magnetic field is 56.25 mT (which is of the order of magnitude of 10 % of the trapped magnetic field). The durations of this transverse pulse are 500 s, 50 s, 5 s, and 0.5 s corresponding to dB_{app}/dt of 0.225 mT/s, 2.25 mT/s, 22.5 mT/s and 225 mT/s respectively. The measurements are recorded for 15 min and are presented in Fig. 3(a). On this figure, we plot an additional curve (white circles) showing the trapped field decay ("natural relaxation") expected without any transverse ac magnetic field. This curve is extrapolated from the measurements carried out before the application of the magnetic field (i.e. between t = 300 s and t = 2100 s) by using Eq. (2).

After one triangular pulse, the trapped magnetic induction is reduced by 4.3 %, 2.8 %, 1.8 % and 1.2 % respectively for $|dB_{app}/dt|$ of 0.225 mT/s, 2.25 mT/s, 22.5 mT/s and 225 mT/s. After

Author Postprint of the paper published in Physica C 512 (2015) 42–53
The Publisher version can be found at the following doi:10.1016/j.physc.2015.03.005

this decay and when no transverse ac magnetic field is further applied, the decay rate is measured to be several times less than the natural relaxation decay rate.
The results of a full 3D FEM model of these experiments, using an $E(J)$ power law (Eq. (1)) and field-dependent J_c (Eq. (4)), is shown in Fig. 3(b). The superconducting parameters (n and $J_c(B)$) used are those obtained by fitting on experimental hysteresis loop measured at $T = 77$ K using a Physical Property Measurement System from Quantum Design (PPMS). The procedure yields $n = 37$, $J_{c0} = 4.21\ 10^8$ A/m^2 and $B_0 = 0.88$ T, for $E_c = 10^{-4}$ V/m. Qualitatively, the modelled decay of the trapped magnetic induction shown in Fig. 3(b) is in excellent agreement with the experimental results shown in Fig. 3(a). The numerical values, however, are smaller than the results obtained experimentally, i.e. decays of 3 %, 2.2 %, 1.6 % and 1.3 % respectively for $|dB_{app}/dt|$ of 0.225 mT/s, 2.25 mT/s, 22.5 mT/s and 225 mT/s.

Because of the small amplitude of the transverse cycle compared to the full penetration field, the penetration of the transverse magnetic field is limited to a thin layer at the periphery of the sample. Therefore we can assume that a zone exists inside the volume of the sample where the azimuthal superconducting currents, that were induced during the axial magnetization process, are unaffected by the transverse field. The 3D FEM modelling is used to calculate, along the z axis, this penetration depth of the transverse magnetic induction, B_x, along the surface of the superconductor. Fig. 4 shows the transverse component of the magnetic field calculated by 3D FEM modelling, for several sweep rates of the applied magnetic field (B_x), along the symmetry axis (z axis) of the superconducting pellet at the vicinity of the top surface ($z \leq 5$ mm) and for the maximal amplitude of the magnetic field ($\mu_0 H_{app} = 56.25$ mT). The plots show the decrease of the transverse magnetic field when it enters inside the volume of the superconducting pellet from the top surface, i.e. from $z = 5$ mm to $z = 4.3$ mm. At the centre of the top surface ($z = 5$ mm), the local value of the transverse field (~ 90 mT) is larger than that of the applied field (56.25 mT) by a factor of 1.65 because of demagnetization effects. We can see that the average slope of the curves showing the penetration of the transverse magnetic field inside the sample increases slowly when the sweep rate of the applied field increases. Accordingly, the distance over which the transverse component of the magnetic field decays from its maximal value at $z = 5$ mm to zero, i.e. the penetration depth of the transverse magnetic field, decreases when the sweep rate increases. Notice that for computational resources, the number of nodes in our 3D modelling should be kept smaller than 150,000. As a consequence, the small negative values below $z = 4.5$ mm are numerical errors caused by a larger size of elements below 4.5 mm. Quantitatively, numerical modelling can give the penetration depths of the transverse cycle by calculating the intersection of the linear part of the B_x profile with $B_x = 0$. The penetration depths equal to 0.63 mm, 0.6 mm, 0.57 mm and 0.56 mm for $|dB_{app}/dt|$ of 0.225 mT/s, 2.25 mT/s, 22.5 mT/s and 225 mT/s respectively.

Notice that in this 3D FEM modelling, we consider an isotropic J_c while in ReBCO materials the J_c anisotropy, $J_c^{ab\text{-plane}} / J_c^{c\text{-axis}}$, equals approximately 3. In the case of a J_c anisotropy, we can assume that the penetration from the cylindrical lateral surface (and in particular in the median plane) will be larger than in the case of an isotropic J_c. Therefore, the J_c anisotropy, and the subsequent larger penetration from the lateral surface, could probably be the reason why the demagnetization measured experimentally is slightly larger than that calculated by modelling with an isotropic $J_c = J_c^{ab\text{-plane}}$.

Author Postprint of the paper published in Physica C 512 (2015) 42–53
The Publisher version can be found at the following doi:10.1016/j.physc.2015.03.005

4.2. Influence of the waveform of the transverse magnetic field on the decay of the trapped field

The importance of dB_{app}/dt on the trapped field decay can also be observed in a second set of experiments by considering two excitations of same maximal amplitude, $\mu_0 H_{app} = 56.25$ mT, and same period, $T = 1000$ s, but having different waveforms: triangular and sinusoidal, as sketched in Figs. 2(a) and 2(b) respectively. While for a triangular waveform, the absolute value of the sweep rate of the applied field ($|dB_{app}/dt|$) is constant, its value varies as a cosine when the waveform is sinusoidal. For both waveforms, the decay of the trapped magnetic induction is measured for 6 h (7200 s) and plotted in Fig. 5 either as a function of the amplitude of the transverse magnetic field (Fig. 5(a)) or as a function of time (Fig. 5(b)). It appears clearly that the decay of the trapped magnetic induction is larger for the sinusoidal waveform. However, as can be seen in Fig. 5(b), the difference between the trapped magnetic induction decays in the case of a triangular or a sinusoidal excitation is measured to equal 2.4 mT after one half-cycle, 2.5 mT after one cycle and 2.3 mT after 200 cycles. This result means that, within the error bar, the difference is constant, giving evidence that the difference between the trapped magnetic induction decays in the case of a triangular or a sinusoidal excitation is mainly due to the initial penetration of the transverse magnetic field during the first half-cycle.

In the inset of Fig. 5(b), we show the evolution of the temperature measured during 6 h. No temperature increase can be noticed. The very small irregularities are attributed to the liquid nitrogen refill.

4.3. 2D magneto-thermal modelling results

In addition to the experimental results given by thermocouple measurements, we carry out 2D magneto-thermal modelling using the Brandt algorithm. The geometry is a slab of finite dimensions along x and y figuring the cross-section of the pellet by a vertical plane. The slab is infinite along the z direction. The magnetic field is applied up to 3 T and removed at 15 mT/s along y to trap a magnetization in zero field cooled conditions. Then, after 1200 s in order to let the trapped magnetic field to relax due to the flux creep, the transverse magnetic field of 50 mT is applied along x at 20 Hz (the maximal amplitude and frequency considered in the experiments). The model takes into account the – possibly anisotropic – thermal conductivity k of the pellet and the convective heat transfer coefficient U. Several couples of parameters were studied and reported in table I.

The case *a* is a reference case with a value of U corresponding to small thermal gradient between the sample and the coolant. The case *b* aims at investigating the effect of anisotropy of the thermal conductivity. The case *c* shows the effect of a large heat draining out of the sample on the temperature increase. The last set of parameters (case *d*) does not correspond to a reported value of U but was studied in order to put in evidence the strong influence of the convective heat transfer coefficient in our experimental work.

In each case, the currents and the magnetic field distributions of a magnetized sample subjected to a transverse AC magnetic field are first modelled without taking into account any self-heating. Secondly, the same simulation is carried out with the calculation of the thermal losses. In this second simulation, after each thermal iteration, the critical current density is updated (i.e. reduced) due to the possible temperature increase of the sample.

Author Postprint of the paper published in Physica C 512 (2015) 42–53
The Publisher version can be found at the following doi:10.1016/j.physc.2015.03.005

Because of the different characteristic times for the magnetic problem and the thermal problem, the numerical resolution is partially decoupled, i.e. the update of the temperatures and the subsequent modification on J_c are calculated after a given number or magnetic field cycles depending on its frequency in order to save calculation time. The modelling ends after 15 times the thermal characteristic time, $\tau_c \sim \rho C_p(Lc^2/k+L_c/U)$, function of the density, the specific heat, the thermal conductivity, the convective heat transfer coefficient and the characteristic length. In the case *a*, $\tau_c \sim 5.4$ s. The results are summarized in Fig. 6 (a-d).

Figure 6 (a) shows, in the case *a*, the magnetization decay with (thin line with circles) and without (thick line) the calculation of losses and the modification of J_c (Left/Top) and the average temperature (Left/Bottom) as a function of the time as well as the final temperature distribution on one half of the sample (Right). First we can see that the average temperature is almost stabilized after a time equal to τ_c (here $\tau_c = 5.4$ s) to a value of 4.6 mK above 77 K. Second, no additional decay of the magnetization due to thermal effect can be observed for this set of parameters. Finally, the temperature inside the volume of the superconductor is non-uniform and the maximal increase (12 mK), corresponding to the maximum of the losses, is located at the edge of the modelled geometry, i.e. along the perimeter of the top and the bottom surfaces of the real superconducting pellet.

In the case *b*, we study how the anisotropy of the thermal conductivity affects the results obtained for the case *a*. As can be observed in Fig. 6 (b), there is no change in the magnetization decay and on the average temperature increase. However the temperature distribution is affected by draining more heat in the *x*-direction than in the *y*-direction. Anyway the maximal temperature is still located at the edge and has the same value of 77.012 K as in the case of an isotropic thermal conductivity.

In the case *c*, we study how a larger convective heat transfer coefficient affects the results obtained for the case *a*. The maximal reported value in the literature was found to be 13000 W/m²K but we choose to increase *U* by a decade in order to enhance this effect. In this case, the characteristic time τ_c equals 2.95 s. As can be seen on Fig. 6 (c), the magnetization decay after 15 s is exactly the same as in the case *a* and there is no difference whether taking into account or not the power losses in the system. The average temperature displays a peak of 0.6 mK above 77 K then decays to 0.4 mK above 77 K because of the large heat draining due to the high value of *U*. This is also observed on the temperature distribution sown in Fig. 6 (c) (Right), where it can be seen that the maximal temperature is located at the edge of the sample and is only 2.5 mK above the temperature of the coolant. An anisotropic thermal conductivity would not change that and the results would be similar to those shown in Fig. 6 (b).

In the case *d*, we consider an artificial case where the convective heat transfer coefficient is lower in such a way that the heat generated at the edge of the modelled surface cannot be as effectively removed out of the sample as in the previous cases. So we have decided to use a value of *U* lowered by a decade in comparison to cases *a* and *b*. We also consider that the thermal conductivity is anisotropic. With $U = 200$ W/m²K and an average thermal conductivity of 10 W/mK, the characteristic time $\tau_c = 29$ s. We can see on Fig. 6 (d) (Left/Bottom) that the time required to stabilize the average temperature (at 52 mK above 77 K) is larger by one order of magnitude in comparison to cases *a* and *b*. The temperature distribution behaves similarly as the case *b* with a larger value of the maximum temperature increase (62 mK above the coolant temperature to be compared to 12 mK in the case *b*). The most important result on this case is the magnetization decay. It can be observed that the

magnetization decay obtained when the temperature increase is taken into account is slightly larger than when the temperature (and therefore the critical current density) is kept constant during the experiment. It gives evidence (i) that our modelling is able to reproduce the effect of this temperature increase and (ii) that the additional decay due to the temperature increase is only a small fraction of the total magnetization decay considering these particular set of parameters. The total magnetization decay after 4000 cycles at 20 Hz is approximately 4% of the magnetization while the contribution due to thermal effects is less than 0.2%.

4.4. Slowdown of the trapped field decay

In a next set of experiments, after recording the natural relaxation between t = 300 s and t = 2100 s, i.e. the decay only due to flux creep processes in absence of transverse magnetic field, the GdBCO pellet is subjected to triangular transverse ac magnetic fields at t = 2100 s for 6 h (7200 s). The magnetic field amplitude is 56.25 mT and the periods are 1000 s (similar to the measurement discussed in section 4.2), 100 s, 10 s and 1s, corresponding to $|\mathrm{d}B_{app}/\mathrm{d}t|$ of 0.225 mT/s, 2.25 mT/s, 22.5 mT/s and 225 mT/s. The results are shown in Fig. 7. The natural relaxation of the trapped field is obtained by fitting each set of data recorded between t = 300 s and t = 2100 s to the logarithmic law expressed in Eq. (2) and all curves are plotted over a duration of 6 h in Fig. 8 (grey curves).

First we can see that the four curves extrapolated from the measurement in the absence of transverse field are very close to each other within a 2 mT error bar, showing that the initial trapped field configuration can be assumed to be identical in each case before the application of the transverse magnetic field. Second we can observe that in the case of higher sweep rates, the initial rate of decay of the trapped field is larger but the slope of the curve tends to decrease more rapidly. Because of the decrease of the slope at high $\mathrm{d}B_{app}/\mathrm{d}t$, a crossover can occur, as can be noticed at t =12000 s for the curves at 225 mT/s and 22.5 mT/s. This feature has to be related to the increase of the current density with the increase of the sweep rate of the applied magnetic field increases, and therefore of the induced electric field (through Faraday's law); as it is the case for the higher slope of the transverse field penetration inside the sample (cf. Fig. 4) and the associated smaller penetration depth for increasing sweep rates of the applied transverse magnetic field.

In order to compare the effects of the various parameters of the transverse fields on the trapped field decay, it is desirable to remove the contribution of the sweep rate dependence of the current density in the experimental data. The best way to proceed is to use the fact that the nonlinear dependence of the $E(J)$ relationship leads to so-called scaling laws [65-67]. These laws state that when the time scale is divided by a factor of C, Maxwell equations are invariant if the magnetic field and the current are both divided by a factor of C to the power $1/(n\text{-}1)$. Such a correction is applied to the measurements carried out at several $|\mathrm{d}B_{app}/\mathrm{d}t|$ presented in Fig. 7 using a two-step procedure: (i) the natural relaxation curve (grey curves in Fig. 7) is first subtracted from the experimental data and (ii) the results are normalized to the amplitude of the triangular ac magnetic field using the scaling law mentioned above (by dividing the results by $B_{max}/(f/f_0)^{1/(n-1)}$ with f the frequency associated to the measurement and the reference frequency f_0 = 1 Hz). The results corrected in this way are shown in Fig. 8, where the results of an additional experiment, carried out at $|\mathrm{d}B_{app}/\mathrm{d}t|$ = 4500 mT/s are added. The decays of the trapped field are plotted either as a function of the number of cycles (a) or as a function of the time (b).

Author Postprint of the paper published in Physica C 512 (2015) 42–53
The Publisher version can be found at the following doi:10.1016/j.physc.2015.03.005

The same treatment is applied to a set of experiment carried out with a sinusoidal magnetic field of smaller amplitude. The maximal amplitude equals 14.14 mT and frequencies range between 1 mHz and 10 Hz. The results are plotted as a function of the number of cycles (a) or as a function of the time (b) in Fig. 9.

After presentation of this detailed set of experimental data for various parameters of small transverse fields, we discuss their implications in the next section.

5. Discussion

5.1. Thermal effects

The measurement of the sample temperature obtained by the two thermocouples placed on the sample surface shows that no self-heating is detected during the experiment even at the highest $|dB_{app}/dt|$ used in the experiments (4500 mT/s). The temperature measured by the thermocouples might be slightly lowered because of the liquid nitrogen. Careful experimental precautions, however, are taken in order to minimize this effect: the soldering is pressed against the surface of the pellet and insulated from the liquid nitrogen by a droplet of GE varnish in such a way that the temperature measured by the thermocouple is well representative of the temperature of the sample.

From the 2D magneto-thermal modelling results presented in section 4.3., in the case of a superconducting sample immersed in liquid nitrogen and subjected to AC magnetic fields having amplitude lower than 50 mT and frequency lower than 20 Hz, we conclude that (i) the maximum power loss is located at the perimeter of the top and the bottom surfaces of the sample and (ii) no effect of self-heating can really affect the demagnetization decay behaviour. The main reason is because of the large convective heat transfer coefficient that drains the heat generated at the border of the pellet out of the sample.

By extrapolation of the results obtained in the case *d* with a value of $U = 200$ W/m²K, we can assume that the part of the decay that can be attributed to the thermal effect will be larger for lower convective heat transfer coefficients (other parameters kept constant). However in the case of pool boiling experiments (i.e. a superconducting sample immersed in liquid nitrogen), no values as low as 200 W/m²K or lower have ever been reported in the literature, so that one can safely conclude that the thermal effects will be negligible in those cases.

It is of practical interest to compare these experimental and modelling results to an order of magnitude of the possible self-heating in the studied $|dB_{app}/dt|$ range obtained with an analytical formula in the limit case of $Bi << 1$. Approximate analytical formulas were derived in one of our previous works [7] in the case of an infinite cylinder subjected to a longitudinal ac magnetic field with the assumption of a Biot number $Bi = U*L_c/k << 1$. When $Bi << 1$, the thermal behaviour of the sample is dominated by the convective heat transfer because the heat conduction inside the sample is so fast that the temperature inside the sample reaches an equilibrium. According to Eq. (24) of Ref. [7], the equilibrium temperature in the axial configuration can be written as:

Author Postprint of the paper published in Physica C 512 (2015) 42–53
The Publisher version can be found at the following doi:10.1016/j.physc.2015.03.005

$$T_{eq} = T_0 + \frac{1}{2}\left[1 - \sqrt{1 - \frac{8\mu_0}{3}\frac{H_{app}^3}{H_{p0}}\frac{fV}{AU(T_c - T_0)}}\right](T_c - T_0) \quad (5)$$

where T_0 and T_c are respectively the temperature of the liquid nitrogen bath, i.e. 77 K, and the critical temperature of the GdBCO, i.e. 93.13 K, f and H_{app} are respectively the frequency and the amplitude of the applied magnetic field, U is the convective transfer coefficient in liquid nitrogen, A is the outer surface of the sample (here 8.25 10^{-4} m^2) and V is the volume of the sample (here 1.77 10^{-6} m^3). We can observe that the thermal conductivity is absent from Eq. (5) because of the approximation $Bi \ll 1$, i.e. corresponding to $U \gg k/L_c$.

In the literature, a wide range of values for the convective heat transfer coefficient can be found, some papers claim that it can even be as high as 10000 W/m²K [10]. If we calculate the Biot number with L_c = 5 mm and various values of U, we find Bi = 0.1 for U = 200 W/m²K, Bi = 1 for U = 2000 W/m²K and Bi = 10 for U = 20000 W/m²K. Then we are at the limit of application of Eq. (5) for U = 200 W/m²K. Using Eq. (5) for a sinusoidal AC magnetic field of 56.25 mT applied longitudinally at the frequency of 20 Hz (same period as the triangular AC field applied at $|dB_{app}/dt|$ = 4500 mT/s), the average temperature increase is limited to 17.6 mK. This value obtained by the analytical 1D model is less than the average temperature calculated by our 2D magneto-thermal model, but the order of magnitude of self-heating is not sufficient to strongly affect the current density inside the sample and then, for this range of magnetic field amplitudes and frequencies, the magnetization decay is approximately the same whether we do take into account the thermal losses or not.

Although the order of magnitude of the temperature increase calculated from Eq. (5) is obtained in the longitudinal configuration, the value is in fair agreement with that obtained in the 2D magneto-thermal modelling. Therefore, Eq. (5) can be used to quickly predict a possible self-heating of the sample regarding the parameters of the applied magnetic field and the superconducting properties of the sample (even if it is not accurate depending on the value of the convective heat transfer coefficient).

To conclude about the thermal effects, from the experimental and modelling results, we can be confident in the fact that for small transverse magnetic fields applied at low frequency, no evidence of additional magnetization decay due to self-heating can be found. Therefore, we attribute all magnetization decays discussed in this work only to the redistribution of the current inside the volume of the GdBCO pellet in order to shield the transverse ac magnetic field.

5.2. Influence of the frequency on the trapped field decay

Results presented in Fig. 3 show that the decay of the maximum trapped field caused by one cycle of transverse field decreases when increasing the sweep rate (or the frequency) of the transverse ac applied magnetic field. From Faraday's law, it follows that the induced electric field in the sample increases, as well as the induced current density, for increasing frequencies. Being larger, the induced currents have to flow on a smaller depth to shield an external transverse magnetic field of a given amplitude. The distribution of superconducting currents, in trapped field and crossed fields configurations, is sketched in a 2D geometry (for simplicity) in Fig. 10. Two cases are compared: (i) low current density and (ii) high current density. This schematic illustration helps understand the sweep rate dependence of the decay of the trapped field discussed above. In a more realistic 3D geometry, one should take into

account that currents do not flow only perpendicular to B_z: the shielding currents opposing to B_x have components parallel to B_z at the periphery of the cylindrical pellet. In spite of this complication, the 3D FEM modelling results, presented in Fig. 4, confirm that the penetration of the transverse ac magnetic field, simulated along the z axis from the top (and the bottom) surface, decreases when the value of $|dB_{app}/dt|$ increases. Therefore, it follows that a larger area of currents flowing azimuthally (sustaining the trapped magnetic induction) is preserved in the volume of the GdBCO pellet.

If we consider that the whole area where the currents have changed direction to oppose the transverse magnetic field does not longer contribute to the z-component of the magnetic induction, the magnetic induction measured at the location of the Hall probe is equivalent to that of a sample whose height has been reduced by two thin layers (one of each side) equal to the penetration depth of the transverse magnetic field. The magnetic induction along the central axis of a cylindrical sample can be calculated by the analytical expression [68]:

$$B_z(z) = \frac{1}{2}\mu_0 J_c \left\{ \left(z+\frac{L}{2}\right) \ln\left(\frac{R+\sqrt{R^2+\left(z+\frac{L}{2}\right)^2}}{\left|z+\frac{L}{2}\right|} \right) - \left(z-\frac{L}{2}\right) \ln\left(\frac{R+\sqrt{R^2+\left(z-\frac{L}{2}\right)^2}}{\left|z-\frac{L}{2}\right|} \right) \right\} \quad (6)$$

This expression is used to calculate analytically what would be the ratio of the magnetic induction at the location of the Hall probe for a sample whose height is reduced by the penetration depth over that of the pristine magnetized sample. For $|dB_{app}/dt|$ of 0.225 mT/s, 2.25 mT/s, 22.5 mT/s and 225 mT/s, and using the penetration depths obtained by the FEM modelling results, the decays calculated with Eq. (6) are found to equal 23.4 %, 22.3 %, 21.6 % and 21.1% respectively, which are several times larger than the decays obtained by the full 3D model as well as the experimental decays. It is important to note that the 3D model is implemented with a field dependent J_c while Eq. (6) is assuming a constant J_c. The field dependence of the critical current density might be the cause of the quantitative disagreement between these analytical results and the measurements. From the above considerations, we can conclude that the simple assumption of a uniformly reduced volume in which the currents are azimuthal is too strict to accurately estimate the magnetization decay. However it gives us an upper bound that can be refined by taking into account the actual current distribution due to the 3D geometry and the field dependence of the critical current density.

5.3. Influence of the waveform

Next we examine the influence of the waveform on the transverse magnetic field on the trapped field decay. For a sinusoidal applied field, because of the smaller sweep rate of the magnetic field when it reaches its maximum, the corresponding value of the induced current density decreases. This leads to a larger penetration of the field inside the volume of the superconducting pellet. Therefore, an additional decay of the trapped magnetic induction occurs even if the maximal amplitude of the transverse ac magnetic field is the same that in the experiment with a triangular waveform. It is worth noticing that this additional decay after the first cycle is the same as that measured after a very large number of cycles, as evidenced by experimental results shown in Fig. 5. FEM modelling carried out over several cycles (not presented here) shows also that, after the first cycle, there is a constant difference of decay for the 4 next cycles between the measurements with a triangular and a sinusoidal waveform

applied field. However, the time consumption of a 3D numerical calculation being quite large, it was not possible, in a decent time, to run the modelling for several hundreds of cycles in order to compare to experimental measurements of transverse fields applied over a long period of time.

According to these results, we conclude that in steady-state regime, the behaviour of the superconductor is not strongly affected by the waveform of the transverse ac magnetic field. The difference between different waveforms is mainly due to the first sweep of transverse field.

5.4. Attenuation of the trapped field decay

Knowing that the magnetic flux density at the surface of the sample is affected differently by transverse field sweeps of various rates (dB_{app}/dt) over long times, the question that arises is whether the decay is due primarily to (i) the number of sweeps (whatever the total time) or (ii) the time during which the sweeps are applied (whatever the number of sweeps). The experimental results displayed in Fig. 8 show that, the decay due to the transverse ac magnetic field cannot be expressed in a simple way on the time neither on the number of cycles. By looking closely to Fig. 8(b) showing the evolution of the normalized trapped field decay as a function of the time, we observe that after an initial decay during the first cycle, a decrease of the trapped magnetic induction occurs during a thousand of seconds. Within that range of time, the relation follows a power law as a function of the time. Gradually, an attenuation of the decay rate comes out. Finally, it can be seen on the measurements at the highest $|dB_{app}/dt|$ that the slope of the decay is reduced by more than an order of magnitude. This feature is fundamental because it shows that the decay due to the application of a transverse magnetic field eventually decreases to become negligible in comparison to the logarithmic decay due to the flux creep.

6. Conclusions

We have carried out a large number of experiments in order to characterize the decay of the trapped magnetic induction on a GdBCO pellet when subjected to a transverse ac magnetic field. These experiments were confronted to 3D numerical modelling using a finite element solver (GetDP) with an H formulation. Compared to existing data in the scientific literature, the purpose was to study in detail the regime where transverse fields of very small amplitude are applied over a long period of time. Such experimental conditions are directly relevant to the practical configurations encountered in engineering applications. They however require great care since the very small magnetic induction decrements (e.g. typically less than 10 μT/cycle after 1000 cycles) need to be measured precisely. In spite of these difficulties, good qualitative agreement was found between experiments and modelling. The conclusions that can be drawn with respect to the behaviour of bulk samples subjected to large number of small cycles are as follows.

First, the thermocouples show no evidence of self-heating in that range of amplitude and frequency of the applied field, confirming that the magnetization decay is only due to a redistribution of the currents in the outer parts of the pellet volume. These measurements are supported by 2D magneto-thermal modelling of a slab subjected to crossed fields showing that the temperature increase is not sufficient to affect strongly the magnetization decay in the ranges of amplitude and frequency studied here.

Author Postprint of the paper published in Physica C 512 (2015) 42–53
The Publisher version can be found at the following doi:10.1016/j.physc.2015.03.005

The results show that, for a given number of applied triangular transverse cycles, lower values of dB_{app}/dt induce larger magnetization decays. Depending on the sweep rate, the first cycle of transverse ac field yields a magnetic induction decay between 5 up to 30 % of the total decay observed over 200,000 cycles showing that the initial penetration is crucial in the demagnetization process.

Great care has been taken in order to distinguish the magnetization decay due to the flux creep relaxation (natural decay) and the magnetization decay due to the transverse magnetic excitation (induced decay). For this purpose, we propose to correct the measurement by subtracting the natural decay obtained by fit of Eqs. (2) or (3) from the experimental data prior the application of the transverse field. Nevertheless, in order to compare measurements obtained at several sweep rates of the transverse applied field, which involve different critical current values, we propose an additional procedure of "normalization" based on the scaling laws implied by the $E(J)$ relationship. Both corrections allow us to enhance the effect of the transverse applied field of small amplitudes on the demagnetization process over the intrinsic material behaviour ruled and dominated by the flux creep.

No clear dependence in the time or in the number of cycles has been demonstrated. However our measurements show clearly that the magnetization decay weakens with the time (or the number of cycles). An important feature of practical interest is that, after a very large number of cycles (e.g. $2\ 10^5$ cycles for a triangular ac magnetic field of 56.25 mT at 4500 mT/s or a sinusoidal ac magnetic field of 14.14 mT at 10 Hz), the decay rate of the trapped magnetic induction due to the transverse ac magnetic field becomes strongly attenuated. The number of cycles required to reach what we may call such "attenuated" regime increases when the frequency (or the sweep rate) of the applied field decreases. In this attenuated regime, the applied transverse magnetic field has a negligible impact on the magnetization decay. The observed decrease of the magnetic induction a function of the time at a rate is nearly exclusively due to the relaxation of the superconducting currents due to flux creep only. However, because of the logarithmic character of the natural relaxation decay, the trapped magnetic induction can be eventually considered as a constant for the purpose of the application.

In conclusion, the present experimental work shows that in the range of small amplitudes and low frequencies of transverse applied magnetic field, as it is generally the case in magnetic bearings and rotating machines, a moderate decay of the trapped magnetic field is unavoidable but we can expect that this decay is limited to the order of magnitude of the transverse applied field amplitude as no self-heating of the sample (which could cause a critical current decrease) is observed.

Acknowledgements

We thank the Communauté Française de Belgique for cryofluid, and equipment grants, under reference ARC 11/16-03.

Author Postprint of the paper published in Physica C 512 (2015) 42–53
The Publisher version can be found at the following doi:10.1016/j.physc.2015.03.005

References

[1] M. Tomita, M. Murakami, High-temperature superconductor bulk magnets that can trap magnetic fields of over 17 tesla at 29 K, Nature 421 (2003) 517–520.
[2] S. Nariki, N. Sakai, M. Murakami, Melt-processed Gd–Ba–Cu–O superconductor with trapped field of 3 T at 77 K, Supercond. Sci. Technol. 18 (2005) S126–S130.
[3] J. H. Durrell, C. E. J. Dancer, A. Dennis, Y. Shi, Z. Xu, A. M. Campbell, N. Hari Babu, R. I. Todd, C. R. M. Grovenor, D. A. Cardwell, A trapped field of 3 T in bulk MgB2 fabricated by uniaxial hot pressing, Supercond. Sci. Technol. 25 (2012) 112002.
[4] H. Teshima, M. Morita, T. Arayashiki, T. Naito and H. Fujishiro, 10 T class trapped field properties of a large Gd–Ba–Cu–O bulk superconductor, Physics Procedia 45 (2013) 61–64.
[5] M. Morita, M. Tanaka, T. Sasaki, M. Hashimoto and K. Sawano, Magnets made of QMG crystals, in Advances in Superconductivity IV - Proceedings of the 4th International Symposium on Superconductivity (ISS ’91), edited by H. Hayakawa and N. Koshizuka, Springer, (1992) 447-450.
[6] P. Laurent, J. F. Fagnard, N. Hari Babu, D. A. Cardwell, B. Vanderheyden and P. Vanderbemden, Self-heating of bulk high temperature superconductors of finite height subjected to a large alternating magnetic field, Supercond. Sci. Technol. 23 (2010) 124004.
[7] P. Vanderbemden, P. Laurent, J. F. Fagnard, M. Ausloos, N. Hari Babu and D. A. Cardwell, Magneto-thermal phenomena in bulk high temperature superconductors subjected to applied AC magnetic fields, Supercond. Sci. Technol. 23 (2010) 075006.
[8] P. Laurent, J. P. Mathieu, B. Mattivi, J.-F. Fagnard, S. Meslin, J. G. Noudem, M. Ausloos, R. Cloots and P. Vanderbemden, Study by Hall probe mapping of the trapped flux modification produced by local heating in YBCO HTS bulks for different surface/volume ratios, Supercond. Sci. Technol. 18 (2005) 1047-1053.
[9] P. Laurent, P. Vanderbemden, S. Meslin, J. G. Noudem, J. P. Mathieu, R. Cloots and M. Ausloos, Measurements of Thermal Effects in a Bulk YBCO Single Domain Superconductor Submitted to a Variable Magnetic Field, IEEE Trans. Appl. Supercond. 17 (2007) 3036-3039.
[10] V. Sokolovsky and V. Meerovich, Heating due to AC losses in high-temperature superconductors, Physica C 308 (1998) 215-220.
[11] I. V. Baltaga, N. M. Makarov, V. A. Yampol'skii L. M. Fisher, N. V. Il'in and I. F. Voloshin, Collapse of superconducting current in high-Tc ceramics in alternating magnetic field, Phys. Lett. A 148 (1990) 213–216.
[12] O. Tsukamoto, K. Yamagishi, J. Ogawa, M. Murakami and M. Tomita, Mechanism of decay of trapped magnetic field in HTS bulk caused by application of AC magnetic field, Journal of Materials Processing Technology 161 (2005) 52-57.
[13] J. Ogawa, M. Iwamoto, K. Yamagishi, O. Tsukamoto, M. Murakami and M. Tomita, Influence of AC external magnetic field perturbation on trapped magnetic field in HTS bulk, Physica C 386 (2003) 26-30.
[14] H. Fujishiro, M. Kaneyama, K. Yokoyama, T. Oka and K. Noto, Generated heat during pulse field magnetizing for REBaCuO (RE = Gd, Sm, Y) bulk superconductors with different pinning abilities, Supercond. Sci. Technol. 18 (2005) 158-165.
[15] T. Oka, K. Yokoyama, H. Fujishiro and K. Noto, Temperature rise in melt-textured large grain superconducting bulk magnets during their magnetizing operations, Physica C 460 (2007) 748-749.
[16] T. Oka, K. Yokoyama, H. Fujishiro and K. Noto, Thermal and magnetic behaviors of a melt-textured superconducting bulk magnet in the zero-field-cooling magnetizing process, Supercond. Sci. Technol. 22 (2009) 065014.

Author Postprint of the paper published in Physica C 512 (2015) 42–53
The Publisher version can be found at the following doi:10.1016/j.physc.2015.03.005

[17] T. Oka, D. Ishiduka, J. Ogawa, S. Fukui, T. Sato, K. Yokoyama and A. Murakami, Magnetic and Thermal Properties of HTS Bulk Magnet in the Pulsed-Field Magnetizing Process, Journal of Superconductivity and Novel Magnetism 26 (2013) 1301-1306.
[18] Y. Zushi, I. Asaba, J. Ogawa, K. Yamagishi, O. Tsukamoto, M. Murakami and M. Tomita, Study on suppression of decay of trapped magnetic field in HTS bulk subject to AC magnetic field, Physica C 412–414 (2004) 708-713.
[19] Y. Zushi, I. Asaba, J. Ogawa, K. Yamagishi and O. Tsukamoto, Study on suppression of decay of trapped magnetic field in HTS bulk subject to AC magnetic field, Cryogenics 45 (2005) 17-22.
[20] M. Ciszek, A.M. Campbell, S.P. Ashworth and B.A. Glowacki, Energy dissipation in high temperature ceramic superconductors, Appl. Supercond. 3 (1995) 509.
[21] J. R. Clem, Flux-line-cutting losses in type-II superconductors, Phys. Rev. B 26 (1982) 2463–2473.
[22] P. Vanderbemden, Z. Hong, T. A. Coombs, S. Denis, M. Ausloos, J. Schwartz, I. B. Rutel, N. Hari Babu, D. A. Cardwell and A. M. Campbell, Behavior of bulk high-temperature superconductors of finite thickness subjected to crossed magnetic fields: Experiment and model, Phys. Rev. B 75 (2007) 174515.
[23] I. F. Voloshin, L. M. Fisher and V. A. Yampol'skii, Nonlinear electrodynamics of vortex matter in hard superconductors, Low Temp Phys 36 (2010) 39-58.
[24] Z. Hong, P. Vanderbemden, R. Pei, Y. Jiang, A. M. Campbell and T. A. Coombs, The Numerical Modeling and Measurement of Demagnetization Effect in Bulk YBCO Superconductors Subjected to Transverse Field, IEEE Trans. Appl. Supercond. 18 (2008) 1561-1564.
[25] P. Vanderbemden, Z. Hong, T. A. Coombs, M. Ausloos, N. Hari Babu, D. A. Cardwell and A. M. Campbell, Remagnetization of bulk high-temperature superconductors subjected to crossed and rotating magnetic fields, Supercond. Sci. Technol. 20 (2007) S174-S183.
[26] J. P. Swartz, M. D. McCulloch, R Pecher, L. Prigozhin, Ph. Vanderbemden and S. J. Chapman, Critical State Modelling of Crossed Field Demagnetisation in HTS Materials, in Applied Superconductivity 2003, edited by A. Andreone, G. P. Pepe, R. Cristiano and G. Masullo, Bristol, IOP Series 181(2004) 859-866.
[27] T. Matsushita, Flux pinning in superconductors, Springer (2007) 102-103.
[28] K. Funaki, M. Noda and K. Yamafuji, Abnormal Transverse-Field Effects in Nonideal Type II Superconductors I. A Linear Array of Monofilamentary Wires, Jpn. J. Appl. Phys. 21 (1982) 299-304.
[29] A. Badía-Majós and C. López, Critical-state analysis of orthogonal flux interactions in pinned superconductors, Phys. Rev. B 76 (2007) 054504.
[30] H. S. Ruiz, A. Badía-Majós, Y. A. Genenko, H. Rauh and S. V. Yampolskii, Superconducting wire subject to synchronous oscillating excitations: Power dissipation, magnetic response, and low-pass filtering, Appl. Phys. Lett. 100 (2012) 112602.
[31] C. Romero-Salazar and O. A. Hernández-Flores, Flux-line cutting in rotating type-II superconductors in parallel geometry, J. Appl. Phys. 103 (2008) 093907.
[32] C. Romero-Salazar and F. Perez-Rodriguez, Response of hard superconductors to crossed magnetic fields: elliptic critical-state model, Physica C 404 (2004) 317–321.
[33] L. M. Fisher, A. V. Kalinova, S. E. Savel'ev, I. F. Voloshin, V. A. Yampolskii, M. A. R. LeBlanc and S. Hirscher, Collapse of the magnetic moment in a hard superconductor under the action of a transverse ac magnetic field, Physica C 278 1997 169–179.
[34] L. M. Fisher, A. V. Kalinov, M. LeBlanc, F. Perez-Rodriguez, S. E. Savel'ev, I. F. Voloshin and V. A. Yampolskii, Suppression of the magnetic moment of a hard superconductor under the action of a transverse magnetic field, Physica B 284 2000 863–864.

Author Postprint of the paper published in Physica C 512 (2015) 42–53
The Publisher version can be found at the following doi:10.1016/j.physc.2015.03.005

[35] I. F. Voloshin, A. V. Kalinov, S. E. Savel'ev, L. M. Fisher, V. A. Yampolskii and F. P. Rodriguez, Electrodynamics of hard superconductors in crossed magnetic fields, J. Exp. Theor. Phys. 84 (1997) 592–598.
[36] A. M. Campbell, Flux cutting in superconductors, Supercond. Sci. Technol. 24 (2011) 091001.
[37] K. P. Thakur, M. P. Staines, L. S. Lakshmi and N. J. Long, Numerical Computation of AC Losses and Flux Profiles in High-Aspect-Ratio Superconducting Strips in Perpendicular AC Magnetic Field, IEEE Trans. Appl. Supercond. 19 (2009) 3770-3778.
[38] F. Pérez-Rodríguez, M. A. R. LeBlanc and G. Gandolfini, Flux-line cutting in granular high-Tc and semi-reversible classical type-II superconductors, Supercond. Sci. Technol. 14 (2001) 386-397.
[39] A. Perez-Gonzalez and J. R. Clem, Response of type-II superconductors subjected to parallel rotating magnetic-fields, Phys. Rev. B 31 (1985) 7048–7058.
[40] J. R. Clem, M. Weigand, J. H. Durrel and A. M. Campbell, Theory and experiment testing flux-line-cutting physics, Supercond. Sci. Technol. 24 (2011) 062002.
[41] A. Badia and C. Lopez, Critical state theory for nonparallel flux line lattices in type-II superconductors, Phys. Rev. Lett. 87 (2001) 127004.
[42] E. H. Brandt and G. P. Mikitik, Unusual critical states in type-II superconductors, Phys. Rev B 76 (2007) 064526.
[43] E. H. Brandt, J. R. Clem and D. G. Walmsley, Flux-line cutting in type-II superconductors, J. Low Temp. Phys. 37 (1979) 43–55.
[44] J. Luzuriaga, A. Badía-Majós, G. Nieva, J. L. Giordano, C. López, A. Serquis and G. Serrano, Magnetic relaxation induced by transverse flux shaking in MgB2 superconductors, Supercond. Sci. Technol. 22 (2009) 015021.
[45] M. Baghdadi, H. S. Ruiz and T. A. Coombs, Crossed-magnetic-field experiments on stacked second generation superconducting tapes: Reduction of the demagnetization effects, Appl. Phys. Lett. 104 (2014) 232602.
[46] A. M. Campbell and D. A. Cardwell, Bulk high temperature superconductors for magnet applications, Cryogenics 37 (1997) 567–575.
[47] T. A. Coombs, A. M. Campbell, I. Ganney, W. Lo, T. Twardowski, B. Dawson, Superconducting bearings in flywheels, Mater. Sci. Eng. B 53 (1998) 225–228.
[48] I. Sakai, T. Higuchi, Dynamic properties of magnetic levitation system using high-temperature superconductors, IEEE Trans. Appl. Supercond. 21 (2011) 1515–1518.
[49] F. N. Werfel, U. Floegel-Delor, R. Rothfeld, T. Riedel, B. Goebel, D. Wippich, P. Schirrmeister, Superconductor bearings, flywheels and transportation, Supercond. Sci. Technol. 25 (2012) 014007.
[50] D. Zhou, M. Izumi, M. Miki, B. Felder, T. Ida, M. Kitano, An overview of rotating machine systems with high-temperature bulk superconductors, Supercond. Sci. Technol. 25 (2012) 103001.
[51] J. R. Hull and M. Strasik, Concepts for using trapped-flux bulk high-temperature superconductor in motors and generators, Supercond. Sci. Technol. 23 (2010) 124005.
[52] X. Granados, J. López, R. Bosch, E. Bartolomé, J. Lloberas, R. Maynou, T. Puig, and X. Obradors, Low-power superconducting motors, Supercond. Sci. Technol. 21 (2008) 034010.
[53] H. Fujishiro and T. Naito, Simulation of temperature and magnetic field distribution in superconducting bulk during pulsed field magnetization, Supercond. Sci. Technol. 23 (2010) 105021.
[54] H. Fukai, Y. Kimura, S. Nariki, N. Sakai, M. Izumi and I. Hirabayashi, The effect of inhomogeneous flux penetration into bulk superconductor by pulsed field magnetization, Supercond. Sci. Technol. 18 (2005) 1179-1182.

[55] D. A. Cardwell, M. Murakami, M. Zeisberger, W. Gawalek, R. Gonzalez-Arrabal, M. Eisterer, H. W. Weber, G. Fuchs, G. Krabbes, A. Leenders, H. C. Freyhardt and N. Hari Babu, Round robin tests on large grain melt processed Sm–Ba–Cu–O bulk superconductors, Supercond. Sci. Technol. 18 (2005) S173–S179.
[56] P. Dular and C. Geuzaine, GetDP Reference Manual: The Documentation for GetDP, a General Environment for the Treatment of Discrete Problems (2006) http://www.geuz.org/getdp.
[57] P. Dular, C. Geuzaine, A. Genon and W. Legros, An evolutive software environment for teaching the finite element method in electromagnetism, IEEE Trans. Magn. 35 (1999) 1682.
[58] G. P. Lousberg, M. Ausloos, C. Geuzaine, P. Dular, P. Vanderbemden and B. Vanderheyden, Numerical simulation of the magnetization of high temperature superconductors: a 3D finite element method using a single time-step iteration, Supercond. Sci. Technol. 22 (2009) 055005.
[59] S. J. Hagen, Z. Z. Wang and N. P. Ong, Anisotropy of the thermal conductivity of YBa2Cu307-y, Phys. Rev. B 40 (1989) 9389-9392.
[60] C. Uher, Thermal Conductivity of High-Tc Superconductors, Journal of Superconductivity 3 (1990) 337-388.
[61] M. Matsukawa, T. Mizukoshi, K. Noto and Y. Shiohara, In-plane and out-of-plane thermal conductivity of a large single crystal of YBa2Cu3O7-x, Phys. Rev. B 53 (1996) R6034.
[62] P. Laurent, J.-F. Fagnard, N. Hari Babu, D. A. Cardwell, B. Vanderheyden and P. Vanderbemden, Self-heating of bulk high temperature superconductors of finite height subjected to a large alternating magnetic field, Supercond. Sci Technol. 23 (2010) 124004.
[63] W. Frost, Heat Transfer at Low Temperatures, Plenum Press, New York, 1975.
[64] J. Mosqueira, O. Cabeza, M. X. François, C. Torrón and F. Vidal, Measurements of pool boiling heat transfer from ceramic Y1Ba2Cu3O7-delta superconductors to liquid nitrogen, Supercond. Sci. Technol. 6 (1993) 584-588.
[65] E. H. Brandt, Superconductor disks and cylinders in an axial magnetic field. I. Flux penetration and magnetization curves, Phys Rev B 58 (1998) 6506-6522.
[66] S. Denis, L. Dusoulier, M. Dirickx, Ph. Vanderbemden, R. Cloots, M. Ausloos and B. Vanderheyden, Magnetic shielding properties of high-temperature superconducting tubes subjected to axial fields, Supercond. Sci. Technol. 20 (2007) 192-201.
[67] D. X. Chen, C. Sanchez, A. Navau, Y. H Shi and D. A. Cardwell, Critical current density of melt-grown single-grain Y-Ba-Cu-O disks determined by ac susceptibility measurements, Supercond.Sci. Technol. 21 (2008) 085013.
[68] I.-G. Chen, J. Liu, R. Weinstein and K Lau, Characterization of YBa2Cu3O7, including critical current density J_c, by trapped magnetic field, J. Appl. Phys. 72 (1992) 1013-1020.

Tables

#	Thermal conductivity			Convective heat transfer coefficient	Biot number
		k_x [W/mK]	k_y [W/mK]	U [W/m²K]	Bi
a	Isotropic	10	10	2000 (medium)	1
b	Anisotropic	20	4	2000 (medium)	0.5 – 2.5
c	Isotropic	10	10	20000 (high)	10
d	Anisotropic	20	4	200 (low)	0.05 – 0.25

Table I: Parameters list for the 2D magneto-thermal modelling.

Author Postprint of the paper published in Physica C 512 (2015) 42–53
The Publisher version can be found at the following doi:10.1016/j.physc.2015.03.005

Figure captions

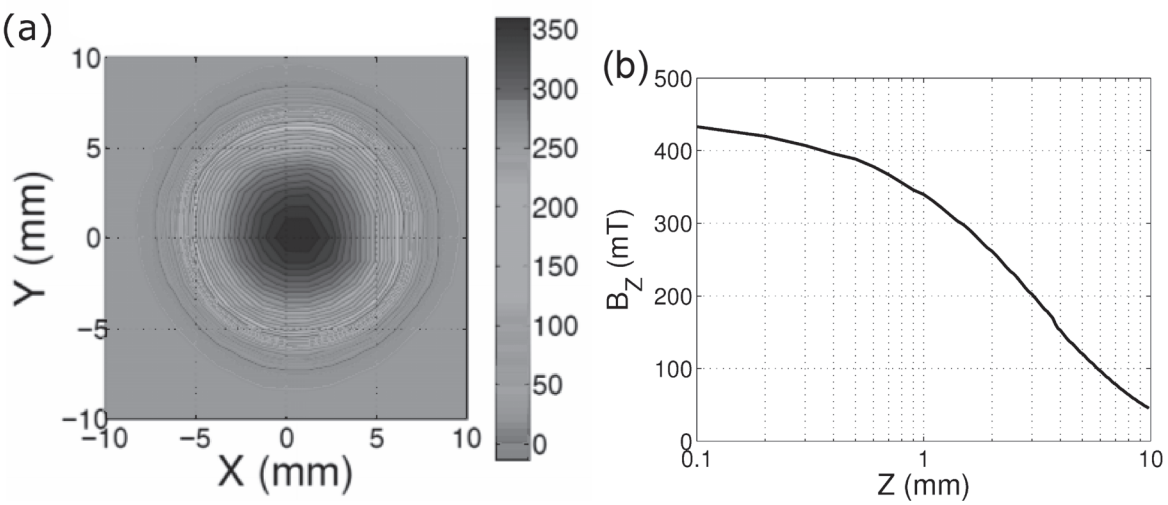

Fig. 1. Trapped magnetic induction of the axially magnetized GdBCO pellet. (a) Distribution of the vertical component of the trapped magnetic induction at z = 500 μm. (b) Trapped magnetic induction as a function of the elevation z above the centre of the GdBCO pellet.

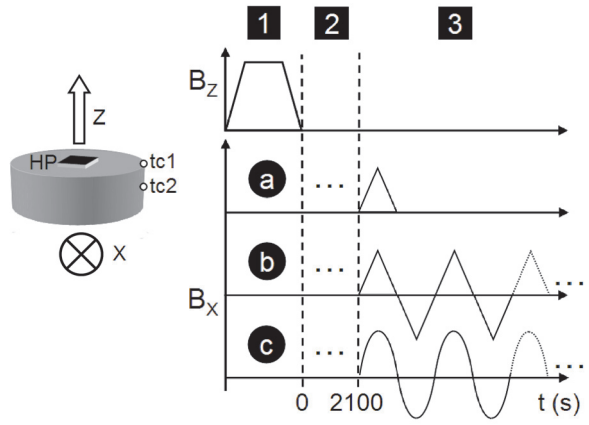

Fig. 2. Left: Schematic picture of the GdBCO sample with the central Hall probe (HP) and two thermocouples (tc1 and tc2). Right: Schematic diagram of the experiments procedure: 1) magnetization of the sample along the z direction, 2) wait for natural relaxation due to flux creep and 3) at t = 2100 s: application of the transverse magnetic field (along the x axis). Three experiments are carried out: (a) one single half cycle of triangular waveform, (b) multiple cycles of triangular waveform and (c) multiple cycles of sinusoidal waveform.

Author Postprint of the paper published in Physica C 512 (2015) 42–53
The Publisher version can be found at the following doi:10.1016/j.physc.2015.03.005

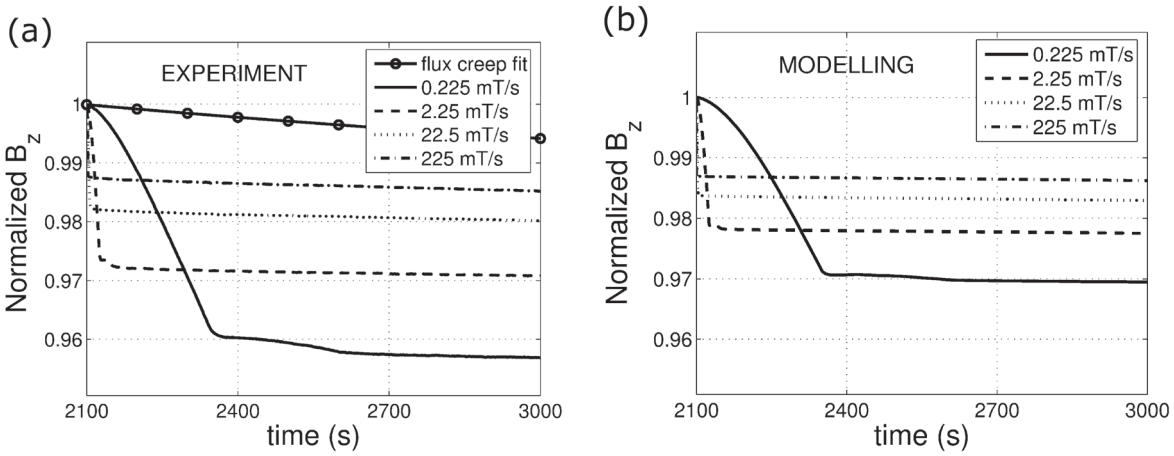

Fig. 3: Decay of the trapped magnetic induction of a GdBCO pellet, magnetized at $t = 0$ s and subjected, at $t = 2100$ s, to a half-period of a triangular ac magnetic field (procedure (a)) having peak amplitude of 56.25 mT and for $|dB_{app}/dt|$ of 0.225 mT/s, 2.25 mT/s, 22.5 mT/s and 225 mT/s. (a) Experimental results with the extrapolation of the decay due to the natural relaxation only. (b) Modelling results at the same sweep rates of the applied transverse magnetic field.

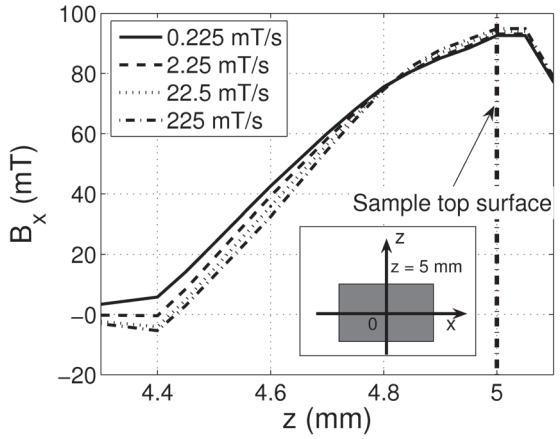

Fig. 4: Penetration profile of the transverse magnetic induction B_x, calculated along the z axis by full 3D FEM modelling on a GdBCO pellet. The sample is magnetized at $t = 0$ s and subjected, at $t = 2100$ s, to a half-period of a triangular ac magnetic field (procedure (a)) having peak amplitude of 56.25 mT and for $|dB_{app}/dt|$ of 0.225 mT/s, 2.25 mT/s, 22.5 mT/s and 225 mT/s. The profiles are plotted for the maximal value of the applied transverse magnetic field.

Author Postprint of the paper published in Physica C 512 (2015) 42–53
The Publisher version can be found at the following doi:10.1016/j.physc.2015.03.005

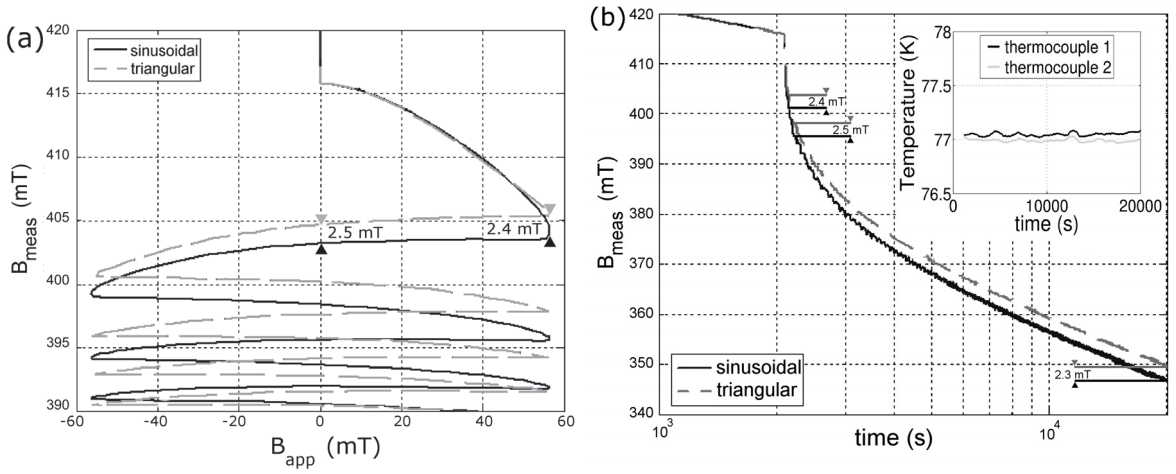

Fig. 5: Comparison of the trapped magnetic induction decay of a GdBCO pellet subjected to sinusoidal (plain) or triangular (dashed) ac magnetic fields having peak amplitude of 56.25 mT and a period of 1000 s. (a) Decay of the trapped magnetic induction as a function of the transverse ac magnetic field. (b) Decay of the trapped magnetic induction as a function of time.

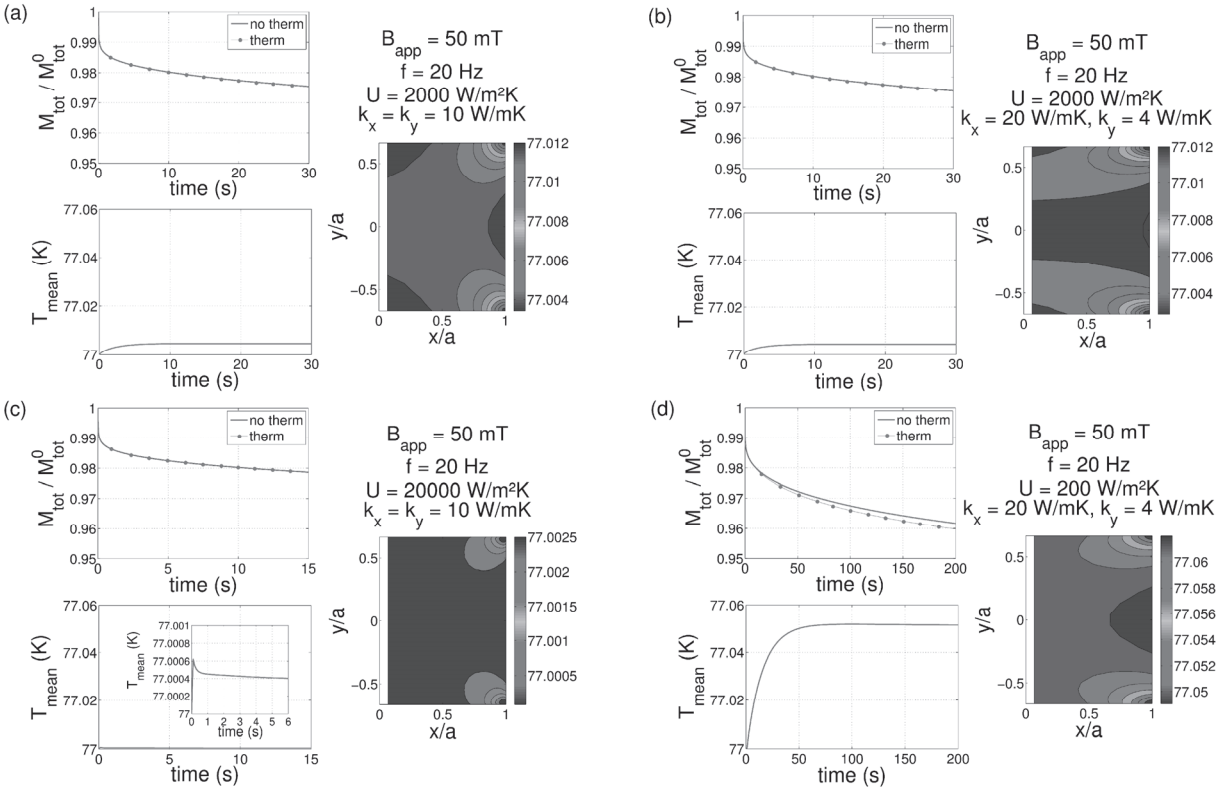

Fig. 6: 2D magneto-thermal modelling using the parameters reported in Table I corresponding to the cases *a* to *d*. The magnetic field is applied along x. In each subfigure, corresponding to each case, we plot: (Left/Top) the magnetization decay with (thin line with circles) and without (thick line) considering the temperature increase due to the dissipated power inside the sample, (Left/Bottom) the average temperature increase over the volume of the sample and (Right) the temperature distribution on one half of the sample.

Author Postprint of the paper published in Physica C 512 (2015) 42–53
The Publisher version can be found at the following doi:10.1016/j.physc.2015.03.005

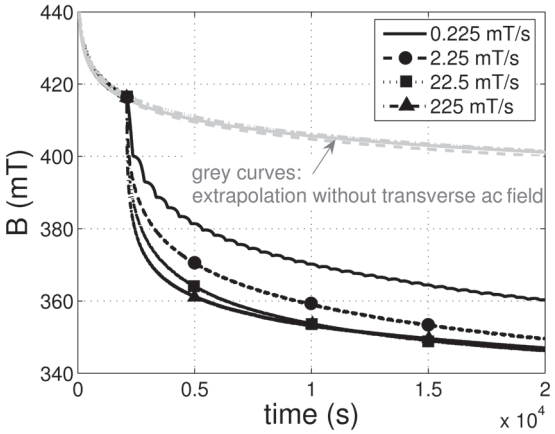

Fig. 7: Decay of the trapped magnetic induction measured on a GdBCO pellet subjected to triangular ac magnetic fields having peak amplitude of 56.25 mT and for $|dB_{app}/dt|$ of 0.225 mT/s, 2.25 mT/s, 22.5 mT/s and 225 mT/s. The grey lines represent the extrapolation of the decay due to the natural relaxation only, obtained from the data between t = 300 s and t = 2100 s when no transverse ac field was applied.

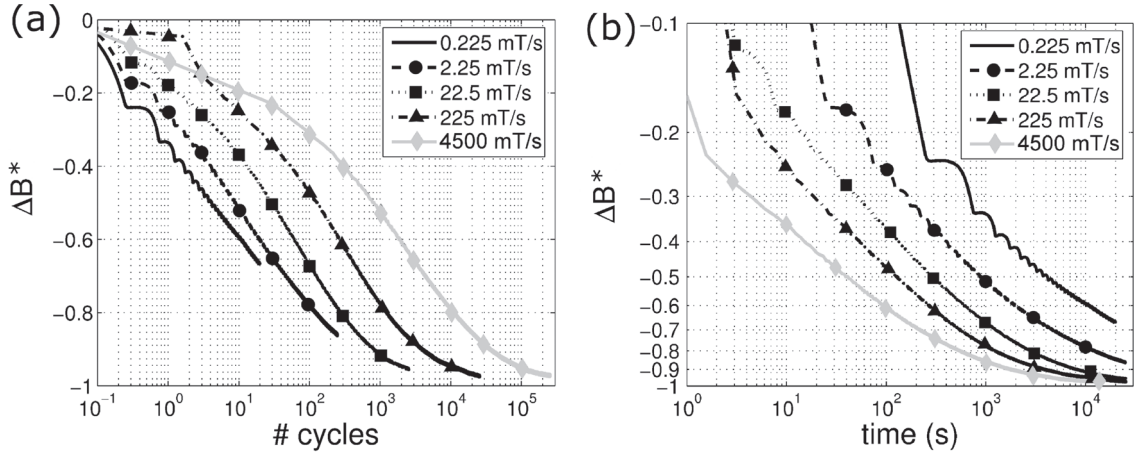

Fig. 8: Decay of the trapped magnetic induction measured on a GdBCO pellet subjected to (a) triangular ac magnetic fields having peak amplitude of 56.25 mT and for $|dB_{app}/dt|$ of 0.225 mT/s, 2.25 mT/s, 22.5 mT/s, 225 mT/s and 4500 mT/s. The figures present, (a) as a function of the number of cycles or (b) as a function of the time, the data after subtraction of the component due to the natural relaxation (flux creep), corrected by the effect of the sweep rate of the magnetic field on the current density and normalized to the maximal amplitude of the triangular ac magnetic field as described in the text.

Author Postprint of the paper published in Physica C 512 (2015) 42–53
The Publisher version can be found at the following doi:10.1016/j.physc.2015.03.005

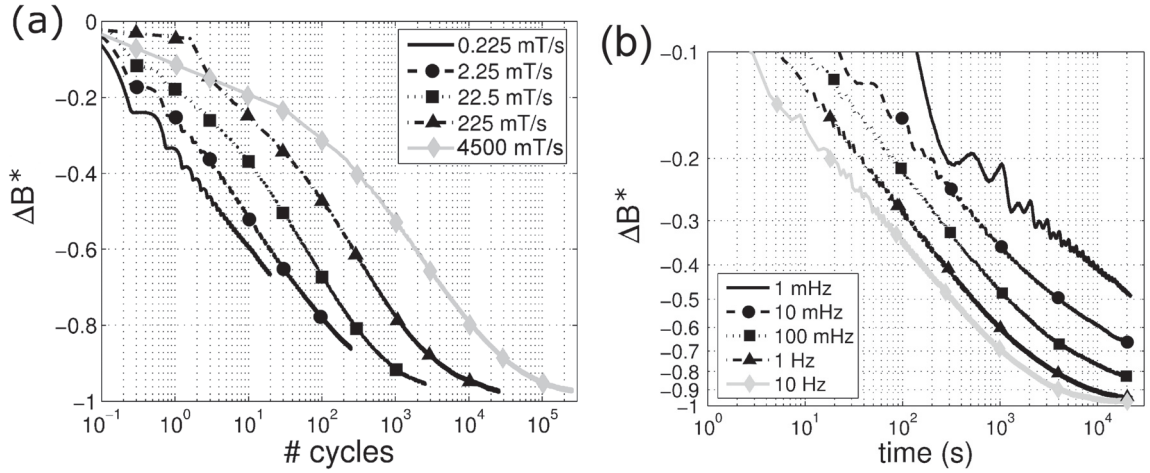

Fig. 9: Decay of the trapped magnetic induction measured on a GdBCO pellet subjected to sinusoidal ac magnetic fields having peak amplitude of 14.14 mT and frequencies ranging between 1 mHz and 10 Hz. The figures present, (a) as a function of the number of cycles or (b) as a function of the time, the data after subtraction of the component due to the natural relaxation (flux creep), corrected by the effect of the sweep rate of the magnetic field on the current density and normalized to the maximal amplitude of the ac magnetic field as described in the text.

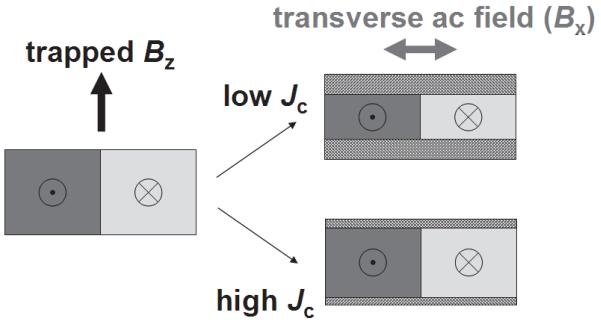

Fig. 10: 2D sketch of the superconducting currents distribution in an axially magnetized GdBCO pellet subjected to a transverse ac magnetic field B_x in the case of low J_c (top) and high J_c (bottom).